

1 Brownian simulations for tetra-gel-type phantom networks composed of prepolymers with bidisperse
2 arm length

3

4 *¹Yuichi Masubuchi, ²Ryohei Yamazaki, ¹Yuya Doi, ¹Takashi Uneyama,
5 ³Naoyuki Sakumichi and ³Takamasa Sakai

6

7 ¹Department of Materials Physics & ²Department of Engineering Physics,
8 Nagoya University, Nagoya 4648603, JAPAN

9

10 ³Department of Bioengineering,
The University of Tokyo, Tokyo 1138654, JAPAN

11

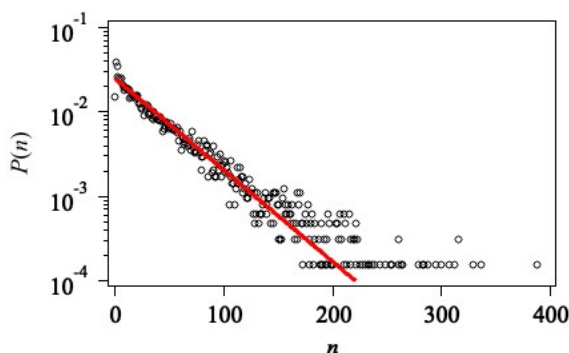
12

13 Supporting Information

14

15 Figure S1 shows the distribution of bead number per strand $P(n)$ for the Rnd networks, which were
16 formed from single long chains via random crosslinking. As expected, the distribution obeys the
17 form $P(n) = (1/n_0)exp(-n/n_0)$, where n_0 is the number averaged bead number and $n_0 = 40$ in this
18 case. The polydispersity index is 2.

19



20

21 **Figure S1** Distribution of bead number per strand $P(n)$ for Rnd. Red solid line shows
22 $P(n) = (1/n_0)exp(-n/n_0)$ with $n_0 = 40$.

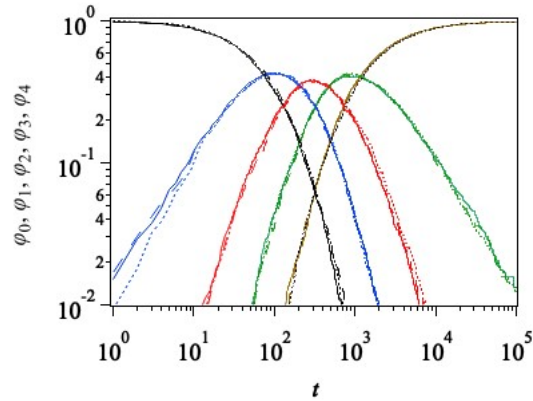
23

24

25 Figure S2 shows the time development of prepolymer fractions with the number of reacted arms of 0
26 to 4. At the beginning of gelation, all the prepolymers are unreacted, and thus, the fraction of
27 polymers with 0 reacted arms, φ_0 , is unity (see black curves). Immediately after the initiation of the
28 reaction, the fraction of polymers with one arm reacted, φ_1 , grows rapidly (see blue curves). φ_1
29 decays after a peak because the reaction occurs for the rest of the arms, and the polymer fractions

30 with 2 or 3 arms are reacted, φ_2 and φ_3 , grow in turn (see red and green curves). Finally, φ_4 (brown
 31 curves) saturates around unity, reflecting that almost all the arms are reacted.

32



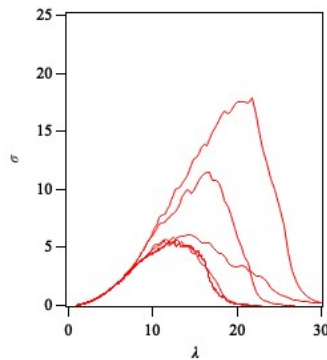
33

34 **Figure S2** Time development of prepolymer fractions having number of reacted arms of 0 (black), 1
 35 (blue), 2 (red), 3 (green), and 4 (brown), for 2a2-3802 (broken curve), s2020 (solid curve), and 1a3-
 36 0525 (dotted curve).

37

38

39 Figure S3 shows the stress-stretch ($\sigma - \lambda$) relation of a s2020 network with various integration step
 40 size, Δt . We have confirmed that the result is insensitive to Δt if we chose the value as $\Delta t \leq 0.002$.



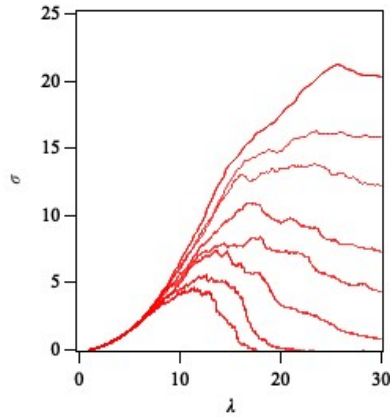
41

42 **Figure S3** $\sigma - \lambda$ relation for a s2020 network with various integration step size, Δt , at 0.02, 0.01,
 43 0.005, 0.002, and 0.001, from top to bottom. The strain rate is 2×10^{-5} .

44

45 Figure S4 shows the $\sigma - \lambda$ relation of a s2020 network with various strain rates. This result clearly
 46 demonstrates that the fracture behavior strongly depends on the stretch rate due to the structural
 47 relaxation induced by bond scissions. We observed that the strain rate dependence became not large
 48 in comparison to the difference among independent simulation runs, if the strain rate is lower than
 49 $\dot{\epsilon} = 2 \times 10^{-5}$.

50



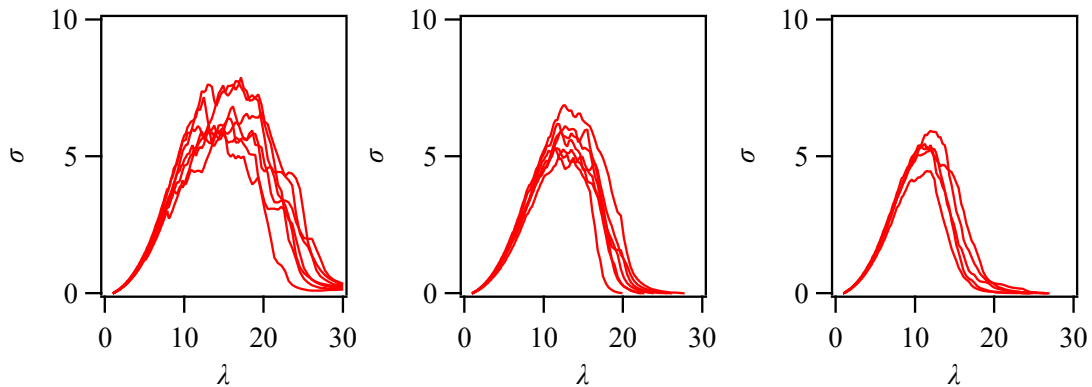
51

52 **Figure S4** $\sigma - \lambda$ relation for a s2020 network with the strain rates at 1×10^{-5} , 2×10^{-5} , 5×10^{-5} ,
 53 1×10^{-4} , 2×10^{-4} , 5×10^{-4} , 1×10^{-3} , and 2×10^{-3} , from bottom to top.

54

55 Figure S5 exhibits the $\sigma - \lambda$ curves for s2020 systems with various system sizes. The involved
 56 prepolymers are 16,400, 32,800, and 65,600, respectively. The scatter among different systems
 57 depends on the system size, and it becomes smaller for larger systems. The stress mitigation after the
 58 peak does not significantly depend on the system size, and the size effect is concealed in the
 59 difference among simulation runs.

60



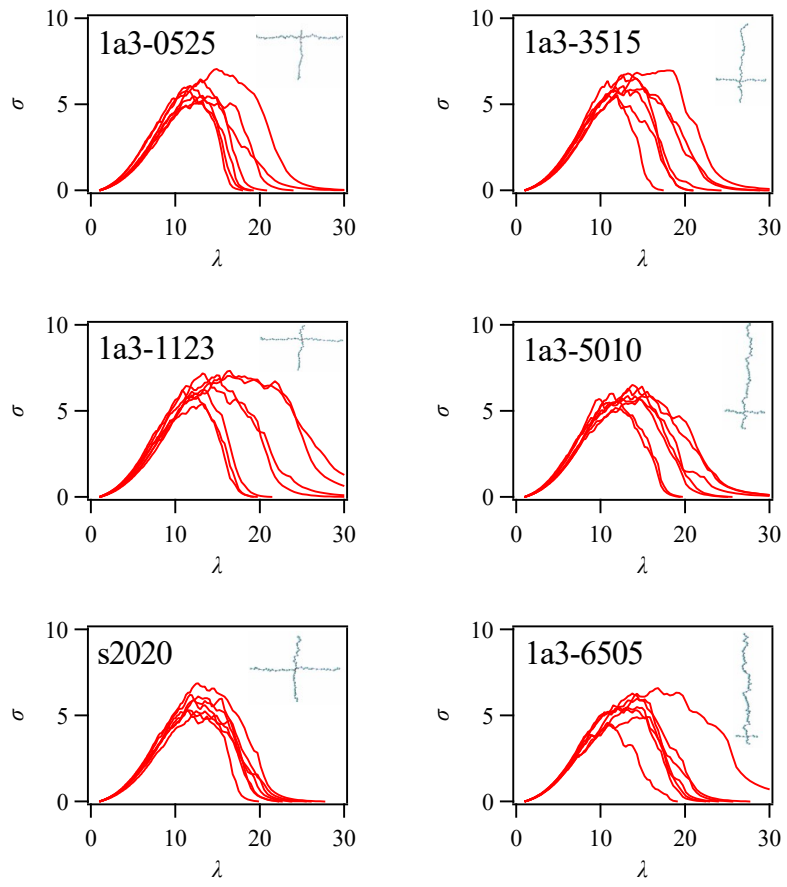
61

62 Figure S5 $\sigma - \lambda$ relation for s2020 systems for eight different simulation runs with the number of
 63 prepolymers of 16,400, 32,800, and 65,600 from left to right. The strain rate is 2×10^{-5} .

64

65 Figure S6 shows the $\sigma - \lambda$ relations for 1a3 systems. As seen for 2a2 systems in Fig 7 in the main
 66 text, the $\sigma - \lambda$ curves for different initial configurations are diverse for the networks made of
 67 asymmetric prepolymers. We observe a few bundles of the $\sigma - \lambda$ curves for some cases in which the
 68 network breakage is dominated by the scission of network strands with specific lengths.

69



70

71 Figure S6 $\sigma - \lambda$ relations 1a3 systems. The results from 8 independent simulation runs are shown.

72